

Bipolar magnetostriction in CoFe_2O_4 : Effect of sintering, measurement temperature, and prestress

Cite as: J. Appl. Phys. **128**, 103904 (2020); <https://doi.org/10.1063/5.0021796>

Submitted: 14 July 2020 . Accepted: 26 August 2020 . Published Online: 11 September 2020

K. Venkata Siva, S. Sudersan , and A. Arockiarajan 



View Online



Export Citation



CrossMark

ARTICLES YOU MAY BE INTERESTED IN

[Magnetic and magnetoelectric response of Gd doped nickel ferrite and barium titanate nanocomposites](#)

Journal of Applied Physics **127**, 114104 (2020); <https://doi.org/10.1063/1.5138239>

[Intrinsic and extrinsic conduction contributions at nominally neutral domain walls in hexagonal manganites](#)

Applied Physics Letters **116**, 262903 (2020); <https://doi.org/10.1063/5.0009185>

[Anisotropy in antiferromagnets](#)

Journal of Applied Physics **128**, 040901 (2020); <https://doi.org/10.1063/5.0006077>



Instruments for Advanced Science

Contact Hiden Analytical for further details:

W www.HidenAnalytical.com

E info@hiden.co.uk

CLICK TO VIEW our product catalogue



Gas Analysis

- dynamic measurement of reaction gas streams
- catalysis and chemical analysis
- molecular beam studies
- dissolved species probes
- fermentation, environmental and ecological studies



Surface Science

- UHV-TPD
- SIMS
- end point detection in ion beam etch
- elemental imaging - surface mapping



Plasma Diagnostics

- plasma source characterization
- etch and deposition process reaction kinetic studies
- analysis of neutral and radical species



Vacuum Analysis

- partial pressure measurement and control of process gases
- reactive sputter process control
- vacuum diagnostics
- vacuum coating process monitoring

Bipolar magnetostriction in CoFe_2O_4 : Effect of sintering, measurement temperature, and prestress

Cite as: J. Appl. Phys. 128, 103904 (2020); doi: 10.1063/5.0021796

Submitted: 14 July 2020 · Accepted: 26 August 2020 ·

Published Online: 11 September 2020



K. Venkata Siva, S. Sudersan,  and A. Arockiarajan^{a)} 

AFFILIATIONS

Department of Applied Mechanics, Indian Institute of Technology Madras, Chennai 600036, India

^{a)}Author to whom correspondence should be addressed: aarajan@iitm.ac.in

ABSTRACT

Magnetostrictive materials are potential candidates for many applications such as sensors, actuators, transducers, and other magnetoelectric applications. Cobalt ferrite (CoFe_2O_4) has proven to be favorable in comparison with commonly used magnetostrictive materials due to its high magnetostriction coefficient and low cost. This work deals with the synthesis of CoFe_2O_4 and subsequent characterization of its magnetostrictive properties. Hydrothermal route was adopted for the synthesis, and the effect of sintering and measurement temperatures on the magnetostrictive response of the synthesized samples was also established. Bipolar magnetostriction has been observed in pure CoFe_2O_4 for the first time, and its control by means of the sintering temperature has been elucidated. The results thus reveal that the temperature is an important parameter in determining the magnetostrictive characteristics of CoFe_2O_4 . The switching from bipolar to unipolar magnetostriction under elevated sintering and measurement temperatures was also observed, and this was owed to the crystal anisotropy of the material. The effect of prestress on the magnetostriction was also studied, wherein it was observed that the application of a compressive prestress resulted in broadening of the magnetostriction loops. The reported bipolar magnetostrictive characteristics are quite interesting and hence can prove to be cost-effective in comparison with existing magnetostrictive materials.

Published under license by AIP Publishing. <https://doi.org/10.1063/5.0021796>

I. INTRODUCTION

Magnetostrictive materials can undergo deformation in the presence of an external magnetic field. These smart materials can thus transform magnetic energy into mechanical and vice versa. This phenomenon is extensively used in many applications such as sensors, energy converters, and actuators.^{1,2} At present, Terfenol-D and Galfenol are the most commonly used magnetostrictive materials for various applications. However, due to the high cost of rare earth elements (Tb and Dy), poor mechanical stability, and limitation of single crystal growth, these materials are less desirable.^{1,3} Recent reports have suggested that expensive conventional magnetostrictive materials can be replaced with magnetostrictive oxides.^{3,4} Polycrystalline CoFe_2O_4 has gained attention because of its moderate room temperature saturation magnetization and magnetostriction, high Curie temperature and coercivity, chemical stability, and high corrosion resistance.^{5–8} This makes CoFe_2O_4 superior for applications in spintronic devices, magnetostrictive sensors, actuators, etc.^{7,8}

A majority of research works have focused on the improvement of the CoFe_2O_4 magnetostrictive properties for use in applications. It is important to note that the properties of CoFe_2O_4 are sensitive to various factors such as synthesis route, sintering temperature, particle size, cation distribution, etc.^{6,8,9} Single crystal CoFe_2O_4 has been shown to provide a maximum magnetostriction of around 600 ppm,^{10,11} which makes it a suitable candidate for replacing existing magnetostrictive materials.^{8,9} A brief survey reveals that many reports on magnetic annealing of CoFe_2O_4 to enhance magnetostriction coefficient have claimed reasonably high magnetostriction.¹² Doping of transition and rare earth elements can also alter the magnetostrictive properties of CoFe_2O_4 .^{13,14} Keswani *et al.* succeeded in this regard by doping with Dy and Mn to enhance the magnetostrictive properties of CoFe_2O_4 .⁸ However, Ghone *et al.* observed a reduction in magnetostriction for Ho doped CoFe_2O_4 .³²

Many groups have synthesized CoFe_2O_4 through different methods such as coprecipitation, tartarate gel, sol-gel, ceramic milling, and ball milling. Bhamre and Joy prepared CoFe_2O_4 using

coprecipitation, auto-combustion, citric gel, and ceramic methods and compared the magnetization and magnetostriction responses of the obtained samples.¹⁶ The auto-combustion method was found to give the highest magnetostriction. Zheng *et al.* synthesized CoFe_2O_4 through the sol-gel method and calcined at 950°C .¹⁷ The synthesized samples were magnetically annealed so as to induce a uniaxial anisotropy and hence a preferential alignment in the samples. Anantharamiah and Joy used the tartarate gel method to synthesize CoFe_2O_4 doped with small amounts of Mg.⁹ This was found to improve the observed magnetostriction. In all of the aforementioned works, the observed magnetostriction was unipolar in nature.

In our earlier work reporting the synthesis of $\text{CoFe}_2\text{O}_4\text{-BaTiO}_3$ core-shell magnetoelectric composites, the CoFe_2O_4 phase prepared by hydrothermal method was found to show a positive magnetostriction at low fields and a negative magnetostriction at higher fields.³ This bipolar magnetostrictive nature has provoked an interest toward a careful characterization of the magnetostrictive properties of CoFe_2O_4 . This bipolar characteristic proves useful in, for example, actuation applications where the need for individual positive and negative magnetostrictive materials is eliminated.

In the present work, CoFe_2O_4 was successfully prepared by hydrothermal synthesis to conduct a detailed study of the existence of bipolar and unipolar magnetostriction. Polycrystalline CoFe_2O_4 was found to exhibit interesting characteristics with sintering and measurement temperatures. The bipolar magnetostriction characteristic in pure CoFe_2O_4 and its transition to a unipolar characteristic with temperature has been reported for the first time in the literature. The effect of measurement temperature and external stresses on the synthesized samples has also been determined by means of experiments.

II. SYNTHESIS

Magnetostrictive CoFe_2O_4 was prepared from aqueous solutions of $\text{Co}(\text{NO}_3)_2 \cdot 6\text{H}_2\text{O}$ and $\text{Fe}(\text{NO}_3)_3 \cdot 9\text{H}_2\text{O}$ through the hydrothermal method. An alkaline pH of 11 was maintained using sodium borohydride and polyvinylpyrrolidone aqueous solutions. The reaction mixture was vigorously stirred for getting a homogeneous solution. Then, the homogeneous solution was transferred to a 50 ml teflon lined stainless steel autoclave, which was closed and allowed to react at a temperature of 120°C for 12 h inside the furnace. After the reaction, the autoclave was allowed to cool naturally at room temperature inside the furnace. The obtained solution was centrifuged 5 times at 10 000 rpm so as to remove water soluble impurities such as sodium salts. The obtained product was dried at 80°C and made into pellets. These pellets were sintered at 700°C , 800°C , 900°C , 1000°C , and 1300°C for 5 h, and these will be referred to as CF7, CF8, CF9, CF10, and CF13 hence forward. A flow chart summarizing the synthesis procedure has also been shown in Fig. 1.

III. EXPERIMENTAL SETUP

The X-ray diffraction (XRD) patterns of the synthesized samples were obtained using a Bruker D8 Discover AXS, X-ray diffractometer. Measurements were performed in the 2θ range of $20^\circ\text{--}80^\circ$ with Co radiation (1.78919 \AA).

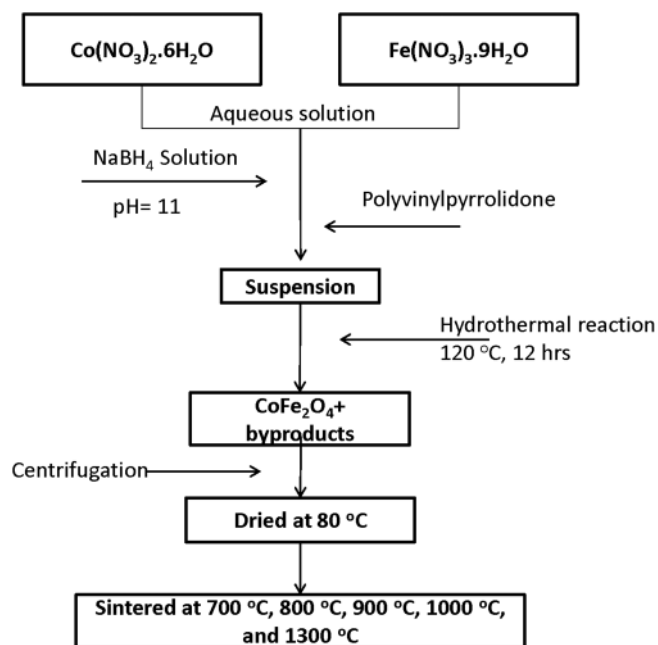


FIG. 1. Flow chart of hydrothermal synthesis procedure.

The magnetostriction was measured for the five different sintered samples (dimensions $13\text{ mm} \times 13\text{ mm}$) at room temperature using a strain gauge pasted along the field direction. A strain indicator (SYSCON 5CH) under quarter-bridge mode was used to monitor the developed strains. A function generator (TEKTRONIX AFG 3022C) was used to generate a quasi-static ramp signal, which was fed to an electromagnet (GMW 5403) through a bipolar power supply (KEPCO BOP 20-20DL). The applied magnetic field was measured by means of a Hall probe connected to a gaussmeter (F.W. Bell Model 6010). The data were acquired by means of a National Instruments Data Acquisition Card (NI USB-6251) using a custom LabView program.

In order to determine the effect of measurement temperature, a temperature-dependent magnetostriction study was also carried out by placing the sample in a specially designed thermal chamber made of stainless steel wrapped with glass wool to prevent the heat dissipation. The desired temperature was maintained inside the chamber by a set of Nichrome heater rods enclosed in a pair of aluminum plates placed at the top and bottom of the chamber. A PID Controller (PFU400) was used to control the current through the heater rods. The temperature inside the chamber was monitored by a K-type thermo couple. A schematic of the experimental setup has been shown in Fig. 2(a).

To determine the effect of external stresses on the magnetostrictive characteristics, magnetostriction measurements under compressive stresses were performed by placing the sample in a sample holder as shown in Fig. 2(c), specially designed to apply loads on the sample in the in-plane direction perpendicular to the applied magnetic field. A load cell (SYSCON 5 kN) was used to

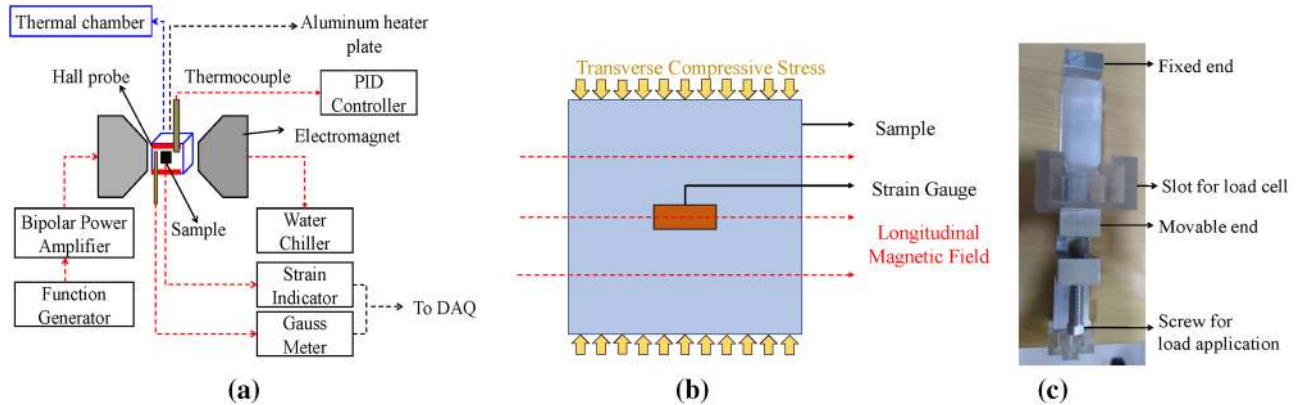


FIG. 2. (a) Schematic of the magnetostriction measurement setup (b) schematic of magnetic field and stress orientations and (c) Photograph of the sample holder for prestress application.

monitor the external load applied to the sample. The sample was placed between the fixed end and the load cell shown in Fig. 2(c). A schematic of the relative orientation of the magnetic field and the compressive stress is shown in Fig. 2(b). The complete setup was placed on a vibration isolation table (SANDVIC COMPONENTS) to prevent unwanted external vibrations. Detailed descriptions of the experimental setup can be obtained from Sudersan and Arockiarajan.¹⁸

IV. RESULTS AND DISCUSSION

Results of X-ray diffraction studies on the CF8 and CF13 samples are summarized in Fig. 3. The XRD patterns are found to match well with the standard JCPDS data of CoFe_2O_4 (JCPDS:

Card No 22-1086) where all the peaks are indexed by corresponding Miller indices. To confirm the phase formation, Reitveld refinement was performed using Fullprof Suite.¹⁹ CoFe_2O_4 was found to be crystallized in cubic spinel structure Fd3m, and no impurity phases were found in the samples prepared. Lattice parameters extracted from Reitveld refinement were found to be 8.38 Å and 8.40 Å for CF8 and CF13, respectively. The lattice constants were calculated for each sintering temperature from the obtained XRD patterns, the results of which are presented in Fig. 3(b). The lattice constant was found to increase with the sintering temperature, which agrees with the observations in previous reports.²⁰⁻²²

Figure 4 depicts the room temperature longitudinal magnetostriction (λ) vs magnetic field (H) loops of CoFe_2O_4 sintered at five different temperatures. Interestingly, in CF7 and CF8 samples, an

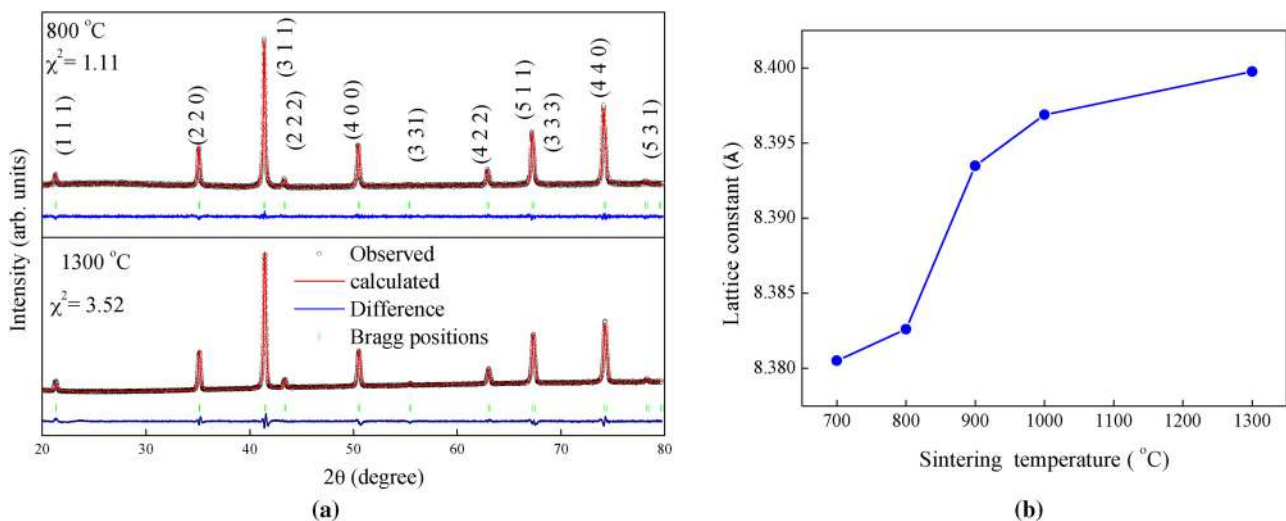


FIG. 3. (a) XRD patterns of sintered samples CF8 and CF13 and (b) lattice constant variation with sintering temperature.

irreversible bipolar (both positive and negative) magnetostriction was observed. Previous reports have shown positive and negative magnetostriction at room temperature in Terfenol D^{1,15} and cation substituted CoFe_2O_4 .² The authors are not aware of any work where pure CoFe_2O_4 was reported to exhibit bipolar behavior.

Previous works utilizing other synthesis techniques such as coprecipitation, sol-gel, auto-combustion method, etc. have reported a unipolar negative magnetostrictive characteristic.^{9,23–26} It can thus be inferred that hydrothermal synthesis coupled with sintering at low temperatures can impart bipolar characteristics to the synthesized CoFe_2O_4 .

In order to confirm this observation and determine the effect of sintering temperature, sintering was also conducted at higher temperatures of 900 °C, 1000 °C, and 1300 °C as specified in Sec. II. The magnetostriction measurements for the same are shown in Figs. 4(c)–4(e). It is seen that the samples sintered at high temperatures (CF9, CF10, and CF13) showed a negative (unipolar) magnetostrictive nature as in previously reported works.²⁵ It is thus confirmed that the bipolar behavior can be attributed to the synthesis technique and the sintering treatment adopted.

Bipolar magnetostriction in CF7 and CF8 and unipolar negative magnetostriction in CF9, CF10, and CF13 characterized by a

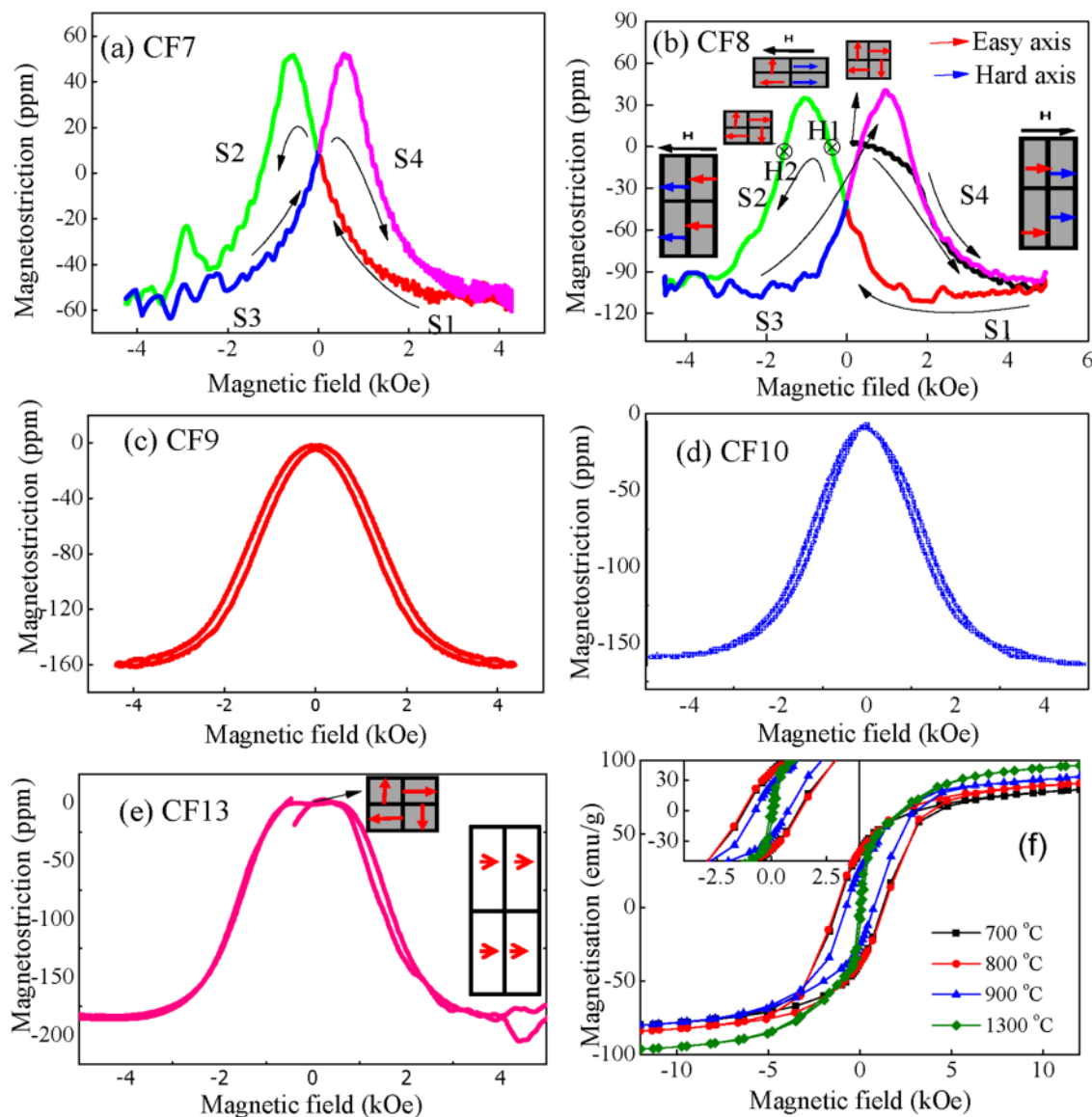
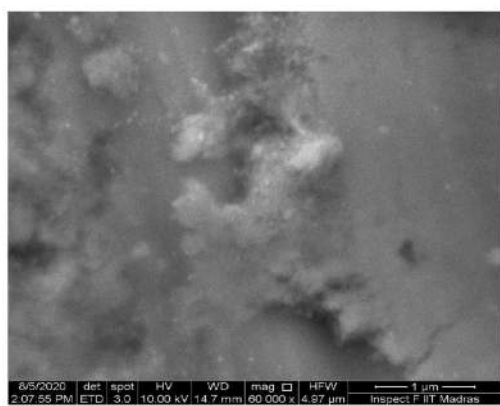


FIG. 4. Magnetostriction curves of samples sintered at (a) 700 °C, (b) 800 °C, (c) 900 °C, (d) 1000 °C, (e) 1300 °C, and (f) M-H loops of sintered samples.

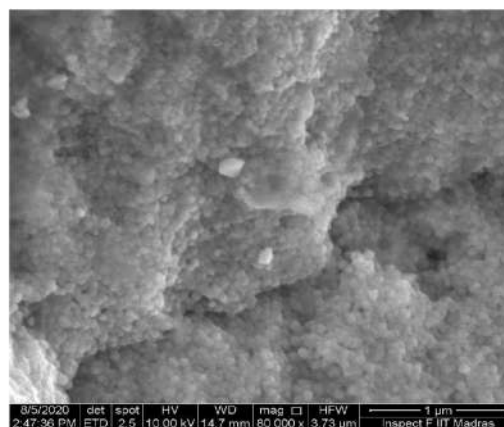
reduced hysteresis loop are two interesting observations from this study. The maximum magnetostriction values (absolute values) observed for CF7, CF8, CF9, CF10, and CF13 samples are 100, 135, 157, 160, and 186 ppm, respectively.

Magnetization measurements were also performed on the heat treated CoFe_2O_4 samples, which revealed an increase in magnetization with heat treatment as shown in Fig. 4. A similar observation was made by Nlebedim *et al.*,²⁷ which was attributed to the redistribution of cations during heat treatment, which increases the Fe^{3+} concentration in octahedral sites, thus leading to an increase in the magnetization. In the current study, the cation distributions calculated from the Rietveld refinement for the CF8 and CF13 samples are $(\text{Co}_{0.222}\text{Fe}_{0.758})[\text{Co}_{0.778}\text{Fe}_{1.215}]_4\text{O}_4$ and $(\text{Co}_{0.249}\text{Fe}_{0.746})[\text{Co}_{0.751}\text{Fe}_{1.227}]_4\text{O}_4$, respectively. Here, round brackets indicate tetrahedral site and square brackets indicate octahedral site. This increase in Fe^{3+} concentration in octahedral sites agrees with the findings of Nlebedim *et al.*²⁷ Sintering at increased temperatures also causes a reduction in the hysteresis in the

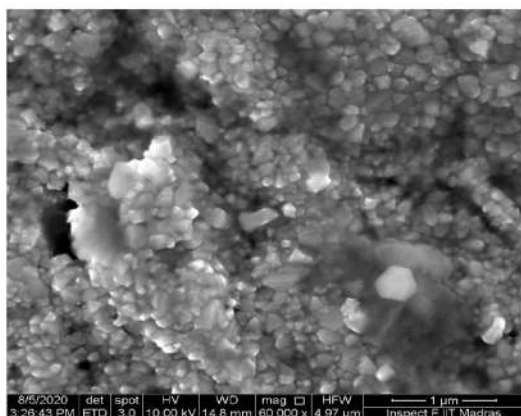
M–H behavior. In order to understand this, FEG-SEM images were obtained for the different samples as shown in Fig. 5. The grain size from the micrographs was calculated using Image J software. The samples sintered at lower temperatures, viz., CF7 and CF8, exhibited fine grain structures whose sizes were found to be less than 20 nm, while those sintered at 900 and 1000 °C exhibited grain sizes of about 0.1 and 0.5 μm , respectively. This clearly indicates that the grain size increases with increasing sintering temperature. The samples with smaller grains showed higher coercivity as compared to those with larger grains as seen from Fig. 5. This can be attributed to the fine grain morphology, which acts as pinning centers causing impediments for the domain movement. However, with the increase in the sintering temperature, formation of larger grains aids an easy path for the domain wall movement, and as a result, the coercivity decreases. This reduction in hysteresis with heat treatment was also observed by Chiu *et al.*²⁸ The magnetization and the magnetostriction results in the current study thus agree with the trends reported in the literature.



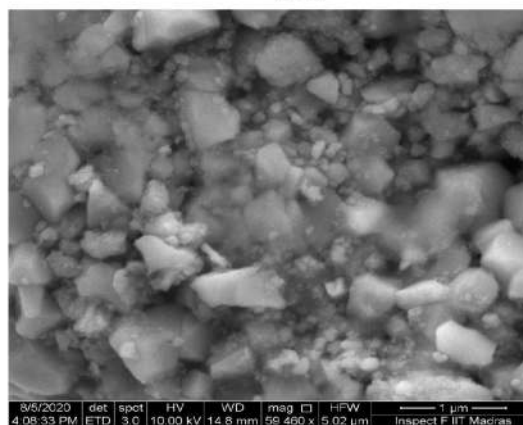
(a)



(b)



(c)



(d)

FIG. 5. SEM images of samples (a) CF7, (b) CF8, (c) CF9, and (d) CF10.

CoFe_2O_4 has two magnetostriction coefficients λ_{100} and λ_{111} along the two crystallographic [100] and [111] axes, respectively, and these are the magnetic easy and hard directions,^{9,25} and note that $\lambda_{100} < 0$ and $\lambda_{111} > 0$ at room temperature. Figures 4(a) and 4(b) illustrate the magnetostriction curve for CF7 and CF8 samples starting from zero magnetic field. As the field initially increases from zero to maximum (represented as a black curve), magnetic domains tend to orient parallel to the applied field from a random state and the contribution from λ_{100} dominates λ_{111} . At saturation, both the easy and hard axis domains orient themselves along the field direction. As the field reduces (S1), the alignment of the domains weakens. At low magnetic field H1, magnetic moments along the easy direction ([1 0 0]) regain their original state, while hard axes moments ([1 1 1]) remain frozen and hence the resulting strains are

positive. On increasing magnetic field further in the negative direction (S2), at a field H2, magnetic moments along [1 1 1] also align back to their original state and attain a random state. Increasing the magnetic field beyond H2 to negative maximum results in complete saturation in the negative direction. The magnetostriction curve from $-H_{max}$ to H_{max} can be explained using the same hypothesis of domain motion. Higher sintered samples CF9, CF10, and CF13 showed a unipolar negative magnetostriction and narrower hysteresis loops compared to CF7 and CF8. Figure 4(e) illustrates schematics of a domain rotation in higher sintered samples. Higher sintering temperatures lead to redistribution of cations, which affects the magnetic moments in the system. At higher temperatures, the thermal energy exceeds the anisotropy energy,^{27,29} which may cause a gradual decrease in the contribution from λ_{111} . Because of this,

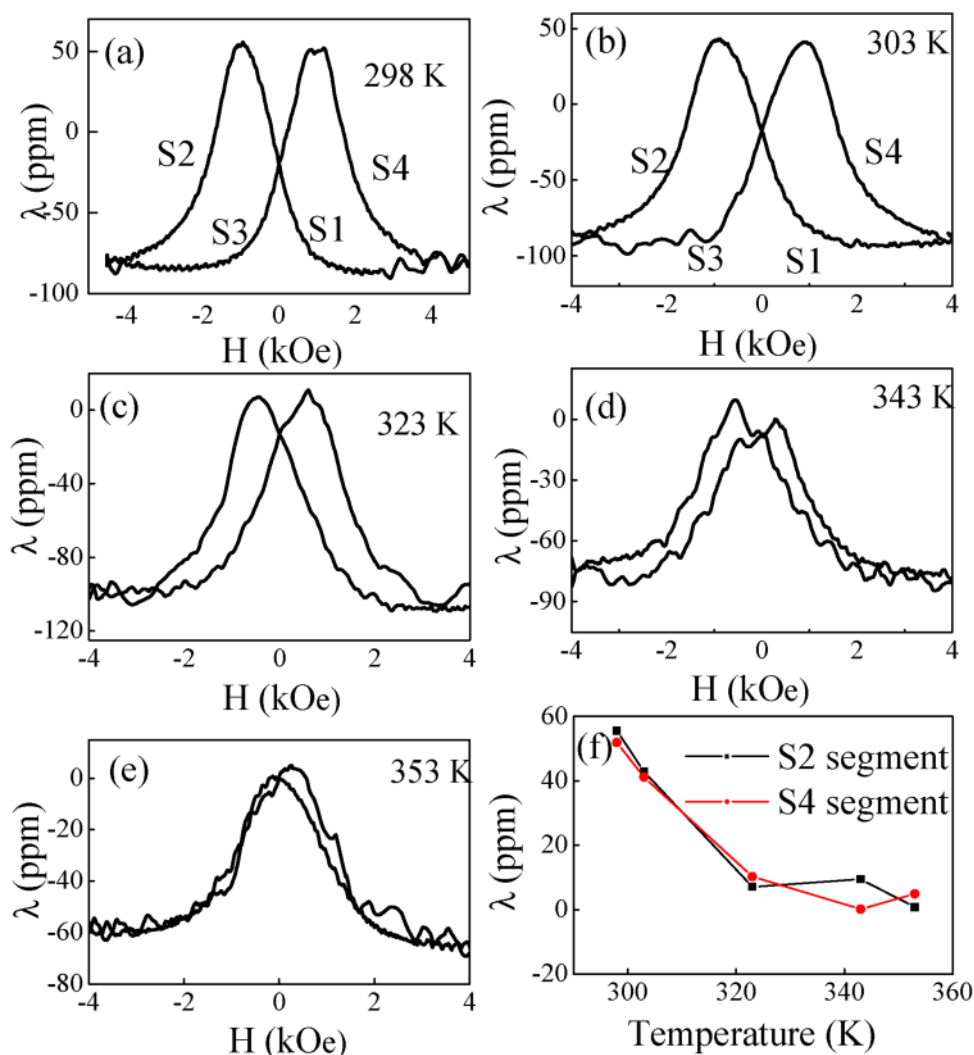


FIG. 6. (a)–(e) Temperature-dependent magnetostriction curves for the CF8 sample and (f) variation of peak magnetostriction of S2 and S4 segments with measurement temperature.

samples sintered at higher temperatures have shown a complete negative magnetostriction with higher magnetostriction values compared to lower sintered samples.

The influence of measurement temperature on the magnetostrictive behavior was further investigated. These measurements were focused on the evolution of the magnetostrictive hysteresis loops and temperature dependence of the magnetostriction of the CF8 sample. Figure 6 shows the magnetostrictive hysteresis loops of CF8, which were measured in the temperature range of 298 K–353 K. The shape of the hysteresis loop, as well as bipolarity of magnetostriction, was retained up to 323 K. However, at temperatures beyond 343 K, the contribution from the positive magnetostriction (λ_{111}) almost diminishes, and the sample shows a fully negative magnetostriction (λ_{100}).

The hysteresis loop area and hence the irreversibility of the loops as well as the maximum magnetostriction are noticeably decreased with an increase in the measurement temperature. The maximum magnetostriction of S2 and S4 segments is shown in Fig. 6(f), which shows a clear decrease of magnetostriction with an increase in the temperature. Besides, the field required for reversing the magnetostriction (H_C) decreased from approximately 1800 Oe at 298 K to 391 Oe at 353 K. Lower magnetization behavior with increasing measurement temperature has been reported previously, which suggests a decrease in the magnetization on approaching the Curie temperature.¹⁸ Thermal fluctuation of magnetic ions and structural defects in the surface arising at high temperatures is determined to be the reason for the lower magnetization.³⁰ At higher temperatures, the contribution from (λ_{111}) decreases as a result of which rotation of domains in the [1 0 0] directions starts to dominate, inducing a switching from bipolar to unipolar magnetostriction.

Since the effect of the sintering and measurement temperature on the magnetostrictive response of the synthesized CoFe_2O_4 has been determined, the effect of stress on the magnetostriction is studied. Figure 7(a) summarizes the effect of a transverse compressive stress on the magnetostriction loop for the CF13 sample. The applied external stress in the perpendicular direction was varied from 0 to 1.5 (kPa). After application of the prestress, the magnetic field is applied longitudinally. An increase in the pre-stress was found to result in the broadening of the magnetostriction vs field loops as seen from Fig. 7(a). The schematic diagram, Fig. 7[b (1)], illustrates randomly distributed domains at zero magnetic field and stress. The application of an external compressive stress results in the rearrangement of domains perpendicular to the applied stress as illustrated in Fig. 7[b (2)]. Application of a magnetic field now induces reorientation of the domains along the field direction. Since a 90° switching is required to align all the domains along the magnetic field, the magnetic field required for switching is greater than that in the absence of stress.^{18,31} The magnetostriction loop thus broadens due to the rotation of domains under an applied pre-stress, higher the stress wider the magnetostriction loop.

The derivative of the magnetostriction curve with respect to the magnetic field (piezomagnetic coefficient) is demonstrated in Fig. 7(c). It is seen that the maximum piezomagnetic coefficient decreases with the application of a compressive prestress. It is also seen that the field at which the maximum slope is attained increases with an increase in prestress.

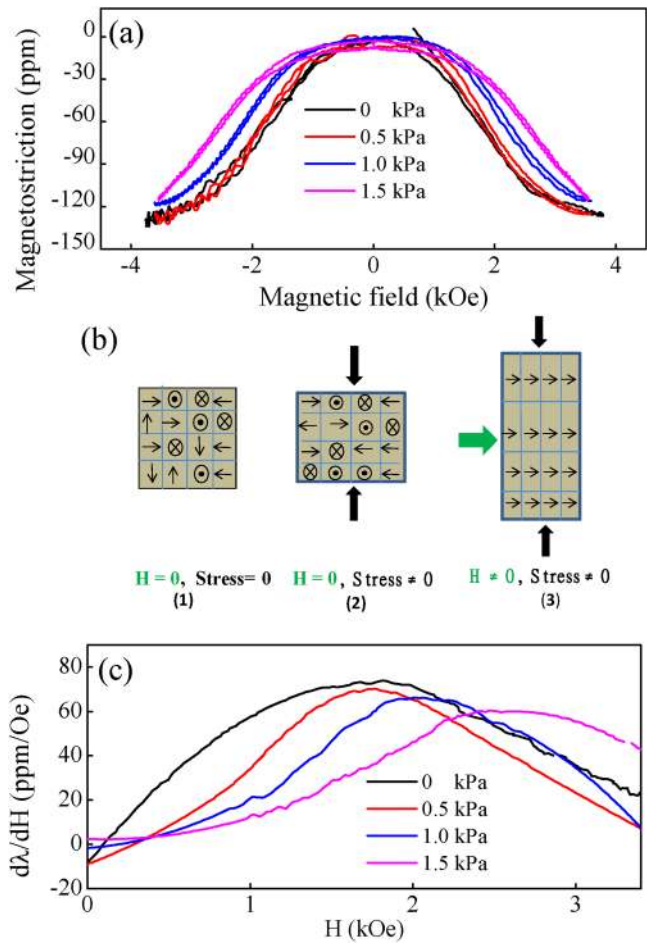


FIG. 7. (a) Magnetostriction curves measured for a CF13 sample at different external compressive stresses, (b) schematic illustration of domain orientation for CF13, and (c) piezomagnetic coefficient at various applied stresses.

V. SUMMARY

Thus, the combined effect of the synthesis route, sintering, measurement temperatures, and external pre-stress on the magnetostriction characteristics of CoFe_2O_4 was determined experimentally. CoFe_2O_4 was synthesized through the hydrothermal route and sintered at different temperatures. Purity of the CoFe_2O_4 phase was confirmed through X-ray diffraction technique. Magnetostriction studies on CoFe_2O_4 revealed the role of the sintering temperature in tuning the magnetostrictive properties of CoFe_2O_4 . Moreover, the measurement temperature also influences the bipolar magnetostrictive nature of CoFe_2O_4 . It can thus be concluded that higher sintering and measurement temperatures favor a unipolar negative magnetostriction. This is due to the strong dependence of anisotropic energy on temperature. Furthermore, application of an external transverse compressive pre-stress was found to result in broadening of the magnetostriction loop and hence a reduction in the piezomagnetic coefficient.

SUPPLEMENTARY MATERIAL

See the [supplementary material](#) that includes the experimental data presented in each figure with appropriate descriptions. Additionally, the XRD data of the other samples are also presented in the [supplementary material](#).

ACKNOWLEDGMENTS

K. V. Siva would like to thank the IITM for providing him the post-doctoral fellowship to conduct this research. The authors also want to thank Professor N. Arunachalam, Department of Mechanical Engineering, and Professor N. V. Ravikumar, Department of Metallurgy and Material Sciences, IIT Madras for their help in obtaining the microstructure images and the XRD data during the COVID-19 pandemic situation. We extend our sincere gratitude to Dr. Arout Chelvane, DMRL, DRDO Hyderabad for fruitful technical discussions and comments regarding the manuscript.

DATA AVAILABILITY

The data that support the findings of this study are available within the article and its [supplementary material](#).

REFERENCES

- ¹J. Gou, X. Liu, K. Wu, Y. Wang, S. Hu, H. Zhao, A. Xiao, T. Ma, and M. Yan, "Tailoring magnetostriction sign of ferromagnetic composite by increasing magnetic field strength," *Appl. Phys. Lett.* **109**, 082404 (2016).
- ²I. Nlebedim, N. Ranvah, Y. Melikhov, P. I. Williams, J. E. Snyder, A. J. Moses, and D. Jiles, "Magnetic and magnetomechanical properties of $\text{Co Al}_x\text{Fe}_{(2-x)}\text{O}_4$ for stress sensor and actuator applications," *IEEE Trans. Magn.* **45**, 4120–4123 (2009).
- ³K. V. Siva, P. Kaviraj, and A. Arockiarajan, "Improved room temperature magnetoelectric response in CoFe_2O_4 - BaTiO_3 core shell and bipolar magnetostrictive properties in CoFe_2O_4 ," *Mater. Lett.* **268**, 127623 (2020).
- ⁴K. K. Mohaideen and P. Joy, "High magnetostriction parameters for low-temperature sintered cobalt ferrite obtained by two-stage sintering," *J. Magn. Mater.* **371**, 121–129 (2014).
- ⁵T. Tatarchuk, I. Mironyuk, V. Kotsyubynsky, A. Shychuk, M. Myslin, and V. Boychuk, "Structure, morphology and adsorption properties of titania shell immobilized onto cobalt ferrite nanoparticle core," *J. Mol. Liq.* **297**, 111757 (2020).
- ⁶R. S. Yadav, I. Kufitka, J. Vilcakova, J. Havlica, J. Masilko, L. Kalina, J. Tkacz, J. Švec, V. Enev, and M. Hajdúchová, "Impact of grain size and structural changes on magnetic, dielectric, electrical, impedance and modulus spectroscopic characteristics of CoFe_2O_4 nanoparticles synthesized by honey mediated sol-gel combustion method," *Adv. Nat. Sci.: Nanosci. Nanotechnol.* **8**, 045002 (2017).
- ⁷B. N. Rao, P. Kaviraj, S. Vaibavi, A. Kumar, S. K. Bajpai, and A. Arockiarajan, "Investigation of magnetoelectric properties and biocompatibility of CoFe_2O_4 - BaTiO_3 core-shell nanoparticles for biomedical applications," *J. Appl. Phys.* **122**, 164102 (2017).
- ⁸B. C. Keswani, S. Patil, Y. Kolekar, and C. Ramana, "Improved magnetostrictive properties of cobalt ferrite (CoFe_2O_4) by Mn and Dy co-substitution for magneto-mechanical sensors," *J. Appl. Phys.* **126**, 174503 (2019).
- ⁹P. Anantharamaiah and P. Joy, "Enhancing the strain sensitivity of CoFe_2O_4 at low magnetic fields without affecting the magnetostriction coefficient by substitution of small amounts of Mg for Fe," *Phys. Chem. Chem. Phys.* **18**, 10516–10527 (2016).
- ¹⁰R. Bozorth, E. F. Tilden, and A. J. Williams, "Anisotropy and magnetostriction of some ferrites," *Phys. Rev.* **99**, 1788 (1955).
- ¹¹R. Bozorth and J. Walker, "Magnetostriction of single crystals of cobalt and nickel ferrites," *Phys. Rev.* **88**, 1209 (1952).
- ¹²S. Indla, A. Chelvane, A. Lodh, and D. Das, "Enhancement in magnetostrictive properties of cobalt ferrite by magnetic field assisted compaction technique," *J. Alloys Compd.* **779**, 886–891 (2019).
- ¹³S. Bhamé and P. Joy, "Magnetic and magnetostrictive properties of manganese substituted cobalt ferrite," *J. Phys. D: Appl. Phys.* **40**, 3263 (2007).
- ¹⁴M. V. Reddy, T. V. Jayaraman, N. Patil, and D. Das, "Giant magnetoelastic properties in Ce-substituted and magnetic field processed cobalt ferrite," *J. Alloys Compd.* **837**, 155501 (2020).
- ¹⁵J. Gou, X. Liu, C. Zhang, G. Sun, Y. Shi, J. Wang, H. Chen, T. Ma, and X. Ren, "Ferromagnetic composite with stress-insensitive magnetic permeability: Compensation of stress-induced anisotropies," *Phys. Rev. Mater.* **2**, 114406 (2018).
- ¹⁶S. Bhamé and P. Joy, "Enhanced magnetostrictive properties of CoFe_2O_4 synthesized by an autocombustion method," *Sens. Actuators A* **137**, 256–261 (2007).
- ¹⁷Y. X. Zheng, Q. Q. Cao, C. L. Zhang, H. C. Xuan, L. Y. Wang, D. H. Wang, and Y. W. Du, "Study of uniaxial magnetism and enhanced magnetostriction in magnetic-annealed polycrystalline CoFe_2O_4 ," *J. Appl. Phys.* **110**, 043908 (2011).
- ¹⁸S. Sudersan and A. Arockiarajan, "Thermal and prestress effects on nonlinear magnetoelectric effect in unsymmetric composites," *Compos. Struct.* **223**, 110924 (2019).
- ¹⁹J. Rodríguez-Carvajal, "Fullprof," Newsletter **26**, 12–19 (2001).
- ²⁰C. Caizer and M. Stefanescu, "Magnetic characterization of nanocrystalline Ni-Zn ferrite powder prepared by the glyoxylate precursor method," *J. Phys. D: Appl. Phys.* **35**, 3035 (2002).
- ²¹S. Ramay, M. Saleem, S. Atiq, S. A. Siddiqi, S. Naseem, and M. S. Anwar, "Influence of temperature on structural and magnetic properties of $\text{Co}_{0.5}\text{Mn}_{0.5}\text{Fe}_2\text{O}_4$ ferrites," *Bull. Mater. Sci.* **34**, 1415–1419 (2011).
- ²²M. Al-Maashani, A. Gismelseed, K. Khalaf, A. A. Yousif, A. Al-Rawas, H. Widatallah, and M. Elzain, "Structural and Mössbauer study of nanoparticles CoFe_2O_4 prepared by sol-gel auto-combustion and subsequent sintering," *Hyperfine Interact.* **239**, 439 (2018).
- ²³Y. Zheng, Q. Cao, C. Zhang, H. Xuan, L. Wang, D. Wang, and Y. Du, "Study of uniaxial magnetism and enhanced magnetostriction in magnetic-annealed polycrystalline CoFe_2O_4 ," *J. Appl. Phys.* **110**, 043908 (2011).
- ²⁴I. Nlebedim, J. Snyder, A. Moses, and D. Jiles, "Anisotropy and magnetostriction in non-stoichiometric cobalt ferrite," *IEEE Trans. Magn.* **48**, 3084–3087 (2012).
- ²⁵I. Nlebedim, N. Ranvah, P. I. Williams, Y. Melikhov, J. E. Snyder, A. J. Moses, and D. Jiles, "Effect of heat treatment on the magnetic and magnetoelastic properties of cobalt ferrite," *J. Magn. Mater.* **322**, 1929–1933 (2010).
- ²⁶V. Giap, R. Groessinger, and R. S. Turtelli, "Magnetoelastic properties of CoFe_2O_4 - BaTiO_3 core-shell structure composites," in *2006 IEEE International Magnetism Conference (INTERMAG)* (IEEE, 2006), pp. 830–830.
- ²⁷I. Nlebedim, Y. Melikhov, and D. C. Jiles, "Temperature dependence of magnetic properties of heat treated cobalt ferrite," *J. Appl. Phys.* **115**, 043903 (2014).
- ²⁸W. Chiu, S. Radiman, R. Abd-Shukor, M. Abdullah, and P. Khiew, "Tunable coexistence of CoFe_2O_4 nanoparticles via thermal annealing treatment," *J. Alloys Compd.* **459**, 291–297 (2008).
- ²⁹A. Franco and F. E. Silva, "High temperature magnetic properties of cobalt ferrite nanoparticles," *Appl. Phys. Lett.* **96**, 172505 (2010).
- ³⁰U. Kurtan, R. Topkaya, A. Baykal, and M. Toprak, "Temperature dependent magnetic properties of CoFe_2O_4 /CTAB nanocomposite synthesized by sol-gel auto-combustion technique," *Ceram. Int.* **39**, 6551–6558 (2013).
- ³¹R. Kellogg, A. B. Flatau, A. Clark, M. Wun-Fogle, and T. A. Lograsso, "Temperature and stress dependencies of the magnetic and magnetostrictive properties of $\text{Fe}_{0.81}\text{Ga}_{0.19}$," *J. Appl. Phys.* **91**, 7821–7823 (2002).
- ³²D. M. Ghone, V. L. Mathe, K. K. Patankar, and S. D. Kaushik, "Microstructure, lattice strain, magnetic and magnetostriction properties of holmium substituted cobalt ferrites obtained by co-precipitation method," *J. Alloys and Compounds* **739**, 52–61 (2018).